The erosion history of the Central Alps: evidence from zircon fission track data of the foreland basin sediments

Cornelia Spiegel[1]*, Joachim Kuhlemann[1], István Dunkl[1], Wolfgang Frisch[1], Hilmar von Eynatten[2] and Kadosa Balogh[3]

[1]*Geologisches Institut, Universität Tübingen, Sigwartstr. 10, D-72076 Tübingen,* [2]*Institut für Geowissenschaften, FSU Jena, Burgweg 11, D-07749 Jena,* [3]*Institute of Nuclear Research of the Hungarian Academy of Science, Bem tér 18/c, H-4026 Debrecen, Hungary*

ABSTRACT

Fission track dating on detrital zircons of Alpine debris in the Swiss molasse basin provides information about the erosion history of the Central Alps and the thermal evolution of source terrains. During Oligocene times, only sedimentary cover nappes, and Austroalpine basement units were eroded. Incision into Austroalpine basement units is indicated by increasing importance of Cretaceous cooling ages in granite pebbles upsection. Erosion of Penninic basement units started between 25 and 20 Ma. Early Oligocene zircon FT ages show that Penninic basement units were exposed at ∼20 Ma. Deeper Penninic units of the Lepontine Dome became exposed first at ∼14 Ma, contemporaneously with the opening of the Tauern window in the Eastern Alps. A middle Miocene cooling rate of 40 °C Myr^{-1} is deduced for the Lower Penninic units of the Lepontine Dome.

Terra Nova, 12, 163–170, 2000

Introduction

Geochronological data obtained from presently exposed rocks yield valuable information about their evolution. However, information on rocks exposed in the geological past is stored in the synorogenic foreland basin sediments. As a result of a closure temperature of about 240 ± 50 °C (Hurford, 1986), zircon fission track (Zr FT) geochronology monitors thermal processes involving approximately the upper 8 km during exhumation of the source areas. Dating of detrital zircons from the foreland basin sediments yields age spectra reflecting the age pattern of different tectonic units exposed in the Central Alps in the geological past. This, in turn, leads to the reconstruction of cooling and exhumation processes during earlier stages of the evolving orogen (see Wagner *et al.*, 1979). Furthermore, the onset of erosion of certain tectonic units can be determined. Comparing FT ages of detrital zircons with those of the recent surface in the source area provides information about the provenance of the siliciclastic material.

The aim of this study is to contribute to the reconstruction of the Oligo-/Miocene denudation history and the thermal evolution of the Central Alps (Switzerland) by fission track dating on detrital zircons from the Swiss molasse sediments.

Correspondence: Tel.: + 49/ 70712974701; Fax: +49 70715059; E-mail: cornelia.spiegel@uni-tuebingen.de

Geological setting

Central Alps

The Alps formed in response to the Tertiary collision between the African and the Eurasian continents. During this collision, the European lithosphere was subducted below the Adriatic plate, which originally acted as a promontory of the African plate. The Penninic units comprise oceanic realms, formerly located between the Austroalpine domain as the northern margin of the Adriatic plate and the Helvetic domain as the southern margin of the European plate (e.g. Schmid *et al.*, 1996 with further references). The Penninic Lepontine Dome dominates the structure of the present-day Central Alps. Only few remnants of Austroalpine upper plate units are preserved in the Central and Western Alps. Penninic and Austroalpine units have highly contrasting cooling age patterns that enable the use of Zr FT dating as provenance indicator: Austroalpine units are generally affected only by Eoalpine Cretaceous metamorphism without any Tertiary overprint. Therefore, they have Zr FT ages older than ∼60 Myr (Hunziker *et al.*, 1992). Penninic units of the Lepontine region reached peak metamorphic conditions of the upper amphibolite facies 38–35 Ma (Jäger, 1973; Steck and Hunziker, 1994). Presently exposed Penninic units belonging to the Lepontine region yield Zr FT ages younger than ∼30 Myr (Hunziker *et al.*, 1992).

Swiss Molasse basin

The Swiss Molasse foreland basin is filled by marine to alluvial conglomerates, sandstones and mudstones. The sedimentary succession is characterized by two coarsening-and shallowing-upward megasequences (e.g. Matter and Weidmann, 1992; Schlunegger *et al.*, 1997). Coarse clastic sedimentation started around 31 Ma with the Lower Marine Molasse stage (UMM) followed by the fluvial sedimentation of the Lower Freshwater Molasse (USM) during Chattian to Aquitanian times. The Burdigalian marine transgression of the Upper Marine Molasse stage (OMM) marks the beginning of the second megasequence. During Langhian to Serravallian times fluvial sedimentation again prevailed and lasted until at least 13 Ma (Upper Freshwater Molasse, OSM). The proximal part of the Swiss Molasse basin is built up of large dispersal systems (from east to the west: Kronberg–Gäbris, Speer, Hörnli, Rigi–Höhrone and Honegg–Napf; see Fig. 1). The sedimentation ages of the Swiss Molasse basin are well-constrained by means of biostratigraphy (Berger, 1992; Bolliger, 1992) and magnetostratigraphy (Kempf *et al.*, 1997; Schlunegger *et al.*, 1997).

The pebble composition of the molasse conglomerates has been studied by Habicht (1945), Matter (1964), Gas-

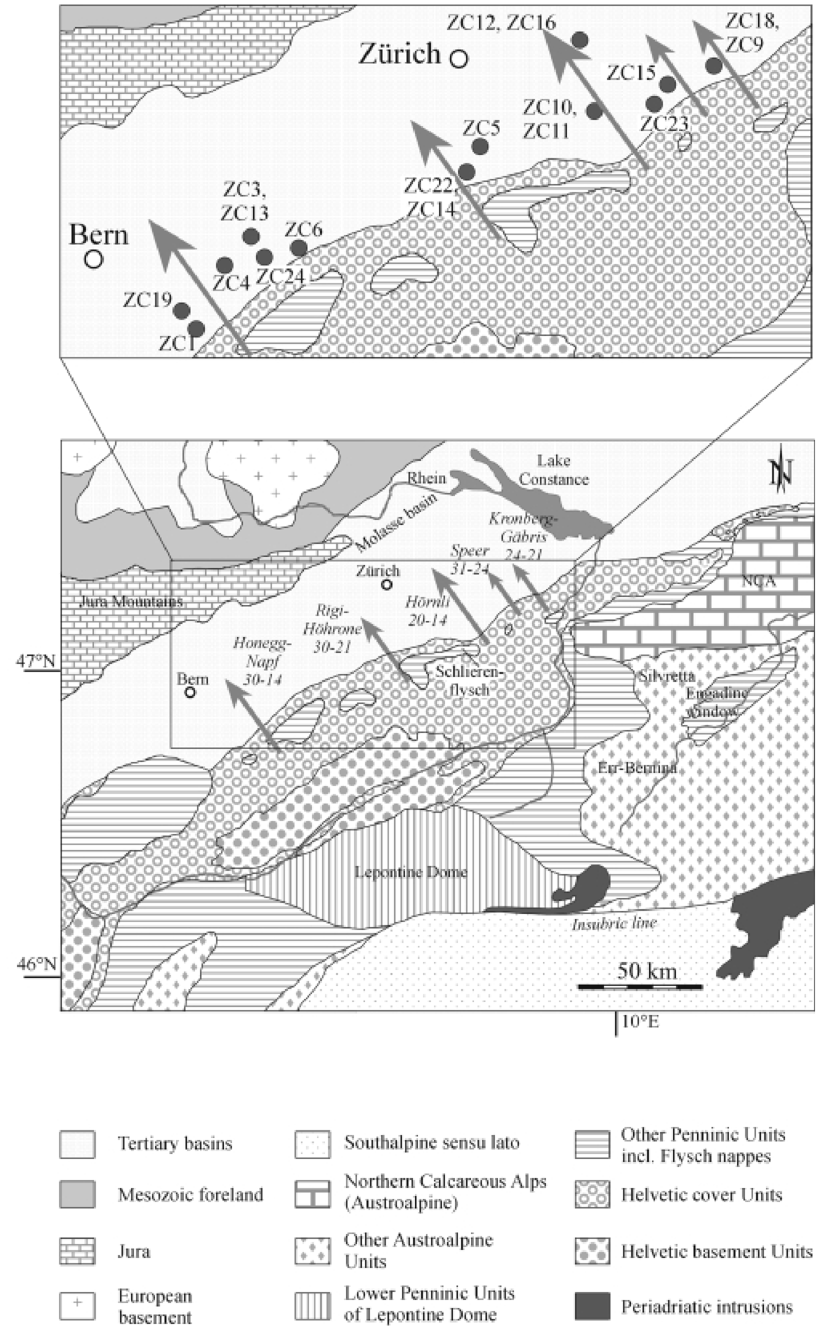

Fig. 1 Simplified geological map of the Swiss Alps and the molasse basin with sample localities. Arrows represent the different dispersal systems, in italics their names and time of activity (Ma) according Schlunegger *et al.*, 1997) and Kempf *et al.* (1997).

ser (1968) and other workers. The clasts of the older conglomerates consist mainly of flysch sandstones, dolomites and limestones. Upsection, the number of crystalline pebbles increases with a maximum around 23 Ma in the Honegg–Napf system (Schlunegger *et al.*, 1998). Granites, granitic gneisses and quartzites are the most abundant crystalline pebbles. The quartzites can be subdivided into two groups, a coarse-grained red Verrucano type and a fine-grained light green quartzite. The latter occurs in sediments younger than 25 Myr old and can make up more than 10% of the components. According to Schlunegger *et al.* (1998), these quartzites are derived from the Middle Penninic Bernhard nappe.

Methods

Twelve sandstones and six pebble populations of different stratigraphic levels of the five main dispersal systems between Bern and Lake Constance were sampled for zircon FT dating (Fig. 1, Table 1). Two approaches were taken: (i) FT dating of detrital zircons from sandstones, which yields age spectra that provide an overview of the cooling histories of the different tectonic units exposed in the catchment areas; (ii) the pebble population dating method (PPD) (Dunkl *et al.*, in review). A pebble population consists of a large number (> 50) of pebbles of the same lithotype and from the same outcrop. They are processed together and dated, yielding an age distribution that reflects the cooling pattern representative for the given lithology. The age distribution shows that if different pebbles of the same lithotype were derived from different tectonic units or from a homogenously cooled source area. Comparing age spectra of sandstones and pebble populations reveals the significance of the dated lithotype for the overall erosion history.

The resulting FT age spectra of sandstones and flysch pebble populations have been modelled with Binomfit (Brandon, 1992). The modelling distinguishes age groups with a Gaussian distribution within one FT age spectrum. Table 2 gives 1σ error and number of grains belonging to the modelled age groups. Of course, age groups with large errors and small number of grains are only of limited geological significance. In this study, all age groups based on less than five grains are neglected. The dated pebble populations, except the flysch pebbles, reveal $P(\chi^2)$-values > 5%, indicating a single population. Therefore, their age distributions were not modelled. In addition to the FT data, micas of crystalline pebbles were dated by the K–Ar method.

Results and discussion

Tables 1 and 2 contain the FT- and modelling-results. Figure 2 shows the stratigraphic and spatial distribution of the dated sandstone samples.

Table 1 Results of the Zr FT dating of sandstones and pebble populations (PPD). n_s, n_i and n_d = number of counted tracks (spontaneous, induced and on dosimeter, respectively), ρ = track densities ($\times 10^5$ tracks cm^{-2}) on grain (ρ_s), print (ρ_i)and dosimeter (ρ_d), $P(\chi^2)$ is the probability of obtaining χ^2 value for v degrees of freedom (where v = number of crystals-1). Ages are calculated using dosimeter glass CN-2 with ζCN-2 = 116.5 ± 1.8. The samples were irradiated in the thermal neutron facility of the Riso reactor (Denmark)

Sample Code	Locality *fan*	Lithology	Sediment age (Myr)	Counted crystals	Spontaneous ρ_s	n_s	Induced ρ_i	n_i	$P\chi^2$ (%)	ρ_d	n_d	Central age (Myr ± 1σ)
ZC 12	Sternberg *Hörnli*	sandstone	13	60	83.3	3672	35.6	1569	0	6.45	12377	86 ± 8
ZC 3	Hengst *H.-Napf*	sandstone	14	57	87.8	4260	67.12	3110	0	4.65	8928	48 ± 4
ZC 4	Eschholzmatt *H.-Napf*	sandstone	19	61	71.5	3880	48.2	2616	0	4.65	8928	39 ± 3
ZC 10	Goldinger Tobel *Hörnli*	sandstone	20	60	153.8	4665	39.7	1204	0	6.45	12377	145 ± 10
ZC 6	Fischenbach *H.-Napf*	sandstone	21	53	126.2	4736	34.4	1292	0	4.65	8928	99 ± 9
ZC 18	Spicher *Kronberg-G.*	sandstone	21	61	229.3	6823	52.5	1561	0	6.62	12343	167 ± 6
ZC 1	Reust *H.-Napf*	sandstone	25	61	143	4378	29.3	896	0	4.65	8928	127 ± 9
ZC 22	Felsenweg *Rigi-H.*	sandstone	26	60	177.9	6439	47.3	1711	0	6.25	12343	140 ± 11
ZC 23	Walensee *Speer*	sandstone	28	60	212.4	6811	40.8	1309	0	6.46	12343	196 ± 11
ZC 5	Zuger See *Rigi-H.*	sandstone	30	76	146.2	6879	29.5	1386	0	4.65	8928	138 ± 11
ZC 24	Waldemme *H.-Napf*	sandstone	30	65	236.1	7118	63.4	1912	0	6.4	12343	145 ± 10
ZC 15	Steintal *Speer*	sandstone	31	54	117.4	4825	40.6	1667	0	6.45	12377	111 ± 10
ZC 16	Sternberg *Hörnli*	Verrucano quartzite (PPD)	13	57	271.6	6804	53.2	1334	26	6.57	12343	193 ± 7
ZC 13	Hengst *H.-Napf*	flysch (PPD)	14	56	114.6	4533	32	1265	0	6.45	12377	135 ± 10
ZC 11	Goldinger Tobel *Hörnli*	red granites (PPD)	20	47	248.8	4633	77.9	1450	9	6.45	12377	119 ± 5
ZC 9	Spicher *Kronberg-G.*	flysch (PPD)	21	59	125.6	4076	25.7	833	0	6.45	12377	177 ± 11
ZC 19	Prässerebach *H.-Napf*	rhyolites (PPD)	26	63	262.7	6682	58.9	1498	6	6.45	12377	168 ± 6
ZC 14	Felsenweg *Rigi-H.*	red granites (PPD)	26	25	245.9	3069	57.9	722	39	6.45	12377	158 ± 7

Middle to late Oligocene evolution

Different sandstones with Oligocene sedimentation (from 31–25 Ma) yield distributions with similar age groups. These age groups can be compared to thermotectonic events which are known from the Austroalpine realm in the Eastern Alps (Frank *et al.*, 1987; Fig. 3). Ages between 240 and 200 Myr are related to the Permo-Triassic crustal extension period, which caused an enhanced heat flow resetting the zircon FT system (see Bertotti *et al.*, 1999). Ages between 170 and 140 Myr have been interpreted to reflect the Jurassic rifting and opening of the Penninic ocean. The high heat flow caused by the rifting affected Austroalpine and South-Alpine units as described by Vance (1999), Bertotti *et al.* (1999), von Eynatten (1996), Dunkl *et al.* (1999). Ages around 80 Myr are widespread in the Austroalpine realm and reflect the cooling period after Cretaceous Eoalpine metamorphism. Another, badly constrained, age group from around 50–40 Ma might be related to a volcanic event documented in the Penninic Schlieren flysch in the Swiss Alps (Winkler *et al.*, 1990) or to the Eocene collision (see, e.g. Schmid *et al.*, 1996).

The age groups discussed in the foregoing paragraph are typical for the Austroalpine realm as documented in the Eastern Alps (Frank *et al.*, 1987). Oligocene molasse sandstones do not contain significant age groups younger than 50–40 Myr. Therefore, the Periadriatic magmatic activity (main period ~30 Ma) did not contribute to the dated Oligocene sediments of the Swiss molasse basin, while, in contrast, many of the Peri-Alpine sedimentary units (e.g. the Apennines, Lombardian flysch, the Austrian molasse basin, Slovenian basin fragments and the Pannonian basin; Dunkl *et al.* 2000) contain

Table 2 Modelled component ages of sandstones and two flysch pebble populations. The modelled ages are calculated using the Binomfit-program (Brandon, 1992), based on the binomial model of Galbraith and Green (1990)

Sample Code	Locality *fan*	Lithology	Sediment age (Myr)	Modelled age groups (Myr ± 1σ) Tertiary	Late Cret.	Early Cret.	Jurassic	> Triassic
ZC 12	Sternberg	sandstone	13	32 ± 2	73 ± 12	126 ± 27	–	282 ± 60
	Hörnli			*n* = 12	*n* = 16	*n* = 23	–	*n* = 9
ZC 3	Hengst	sandstone	14	19.5 ± 0.9	87 ± 4	–	–	–
	H.-Napf			*n* = 24	*n* = 33	–	–	–
ZC 4	Eschholzmatt	sandstone	19	28 ± 1.2	81 ± 5	–	–	–
	H.-Napf			*n* = 39	*n* = 22	–	–	–
ZC 10	Goldinger Tobel	sandstone	20	40 ± 6	86 ± 15	–	148 ± 16	238 ± 42
	Hörnli			*n* = 2	*n* = 7	–	*n* = 35	*n* = 16
ZC 6	Fischenbach	sandstone	21	32 ± 3	67 ± 8	129 ± 13	187 ± 33	–
	H.-Napf			*n* = 8	*n* = 5	*n* = 28	*n* = 12	–
ZC 18	Spicher	sandstone	21	–	–	–	144 ± 12, 195 ± 18	–
	Kronberg-G.			–	–	–	*n* = 29, *n* = 32	–
ZC 1	Reust	sandstone	25	41 ± 9	–	112 ± 9	–	215 ± 26
	H.-Napf			*n* = 3	–	*n* = 37	–	*n* = 21
ZC 22	Felsenweg	sandstone	26	47 ± 3	–	137 ± 10	–	213 ± 17
	Rigi-H.			*n* = 6	–	*n* = 28	–	*n* = 26
ZC 23	Walensee	sandstone	28	–	81 ± 14	165 ± 27	–	240 ± 33
	Speer			–	*n* = 3	*n* = 17	–	*n* = 40
ZC 5	Zuger See	sandstone	30	41 ± 3	–	121 ± 9	–	224 ± 19
	Rigi-H.			*n* = 7	–	*n* = 30	–	*n* = 39
ZC 24	Waldemme	sandstone	30	–	75 ± 4	149 ± 15	–	226 ± 85, 303 ± 86
	H.-Napf			–	*n* = 15	*n* = 28	–	*n* = 11, *n* = 11
ZC 15	Steintal	sandstone	31	54 ± 4	–	100 ± 11	–	213 ± 14
	Speer			*n* = 15	–	*n* = 14	–	*n* = 25
ZC 9	Spicher	flysch (PPD)	21	59 ± 14	–	129 ± 47	–	209 ± 19
	Kronberg-G.			*n* = 3	–	*n* = 11	–	*n* = 45
ZC 13	Hengst	flysch (PPD)	14	–	73 ± 5	140 ± 22	–	219 ± 21
	H.-Napf			–	*n* = 16	*n* = 15	–	*n* = 25

volcanogenic material or euhedral, clear, volcanogenic zircon grains reflecting the Periadriatic magmatism (see also Ruffini *et al.*, 1997, Brügel *et al.*, 2000). Thus, no magmatic bodies of the Periadriatic volcanic edifice (Brügel *et al.*, 2000) were situated in the catchment areas of the rivers draining into the Swiss Molasse basin.

The absence of zircon grains younger than 50–40 Myr in Oligocene Swiss molasse sediments also implies that until the end of the Oligocene no Penninic basement units delivered zircon into the Swiss molasse basin. The occurrence of light green quartzite as components around 25 Ma are not accompanied by a change in the Zr FT age distribution (Fig. f,g). Therefore, they cannot be derived from the Middle Penninic Bernhard nappe as proposed by Schlunegger *et al.* (1998) because such a source is rich in zircon and therefore would have influenced the age distributions of the molasse sandstones. This type of quartzite, however, also occurs in Early Triassic formations in the Austroalpine realm.

Between 31 and 25 Ma the number of young zircons in the sandstones decreases upsection, especially in the eastern part of the basin (Fig. 2). This points to the erosion and recycling of a clastic sediment such as flysch, because an exhuming crystalline mass in the source area would yield increasingly younger ages. Comparison between the age spectra of the molasse sandstones and of two flysch pebble populations (Fig. 4e,f) yield similar age distribution. We therefore conclude that flysch must have been the most important source rock for zircons of Oligocene molasse sandstones. This is corroborated by frequent flysch pebbles in the conglomerates and by light and heavy mineral data (von Eynatten *et al.*, 1999).

The Oligocene sandstones contain a surprisingly high amount of zircon grains with pre-Cretaceous FT ages. These zircon grains may either be inherited from the flysch or from the erosion of crystalline basement unaffected by Cretaceous metamorphism. Figure 4(c,d) shows the age distributions of two crystalline pebble populations. Both samples yield Jurassic age clusters, indicating a source area, which has not been affected by Alpine metamorphism. This is also confirmed by K–Ar dating on micas from several crystalline pebbles (Table 3), which yield late Variscan to Jurassic ages. Therefore, the crystalline basement exposed in the catchment areas of the studied molasse fans during late Oligocene times was widely unaffected by an Alpine overprint.

Early to middle Miocene evolution

Whilst Oligocene sandstones from the different dispersal systems yield similar age distributions, Miocene sands show markedly different patterns. (Fig. 2). Burdigalian sandstones (from *c.* 20 Ma) from the eastern fans (Kronberg–Gäbris, Hörnli) still show a pure Austroalpine age signature with no significant age groups (> 5 grains) younger than 80 Myr old. In contrast, sandstones from the western dispersal sys-

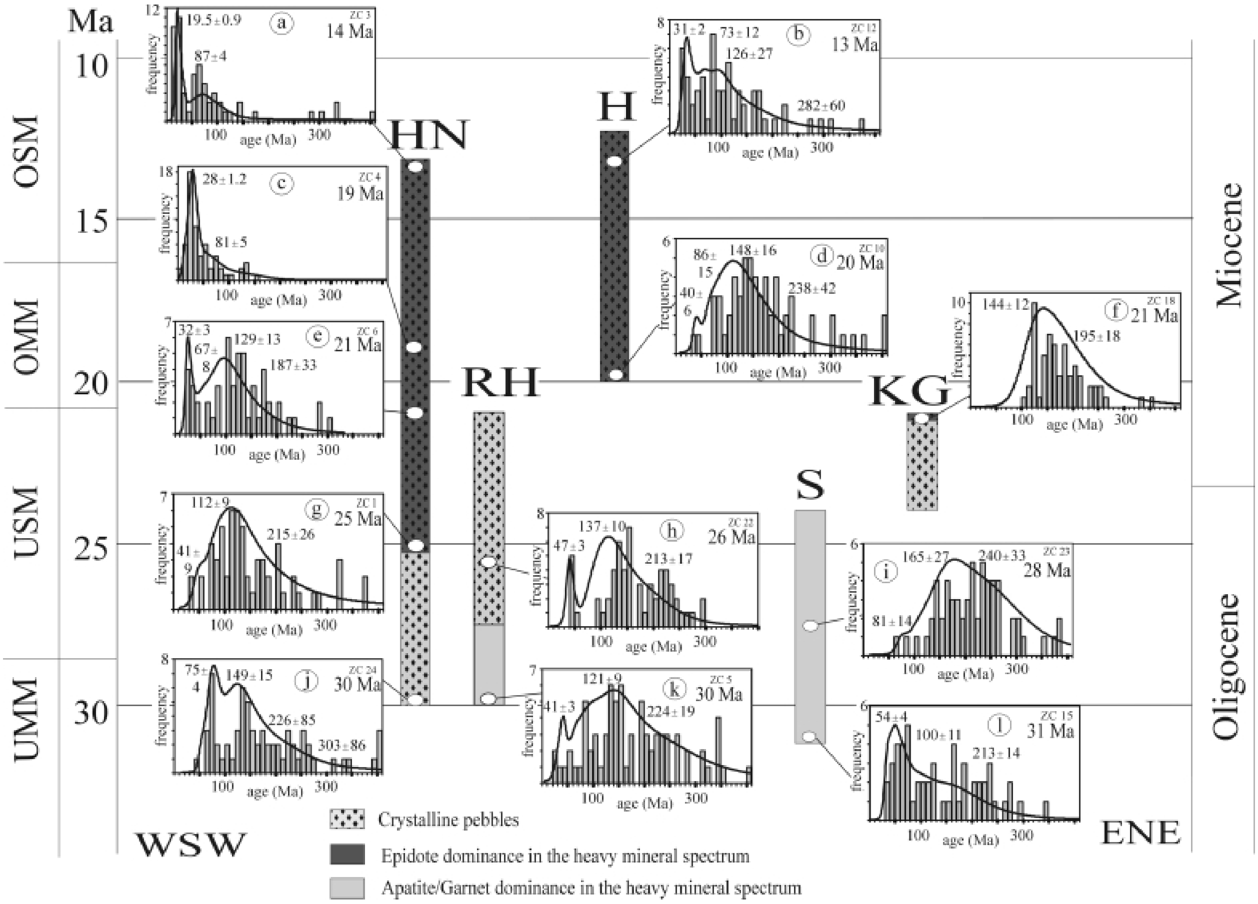

Fig. 2 Stratigraphic and spatial distribution of the dated sandstone samples and the resulting age distributions. FT dating was performed using the external detector method (Fleischer *et al.*, 1964) and the zeta calibration approach (Hurford and Green, 1983). The probability density plots are computed according to Hurford *et al.* (1984). Sedimentation ages and sample codes (ZC number) are at top right, the modelled component ages (Binomfit, Brandon, 1992) are associated with the age groups. The symbolic stratigraphic columns are arranged according to the E–W position of the investigated dispersal systems. The black rhombs indicate the presence of crystalline pebbles, the dark-grey shading epidote dominance in the heavy mineral composition. The vertical axis gives the chronostratigraphic scale and the German abbreviations for the different molasse stages: UMM, Lower Marine Molasse; USM, Lower Freshwater Molasse; OMM, Upper Marine Molasse; OSM, Upper Freshwater Molasse. Dispersal systems: HN, Honegg–Napf; RH, Rigi–Höhrone; H, Hörnli; S, Speer; KG, Kronbergndash;Gäbris.

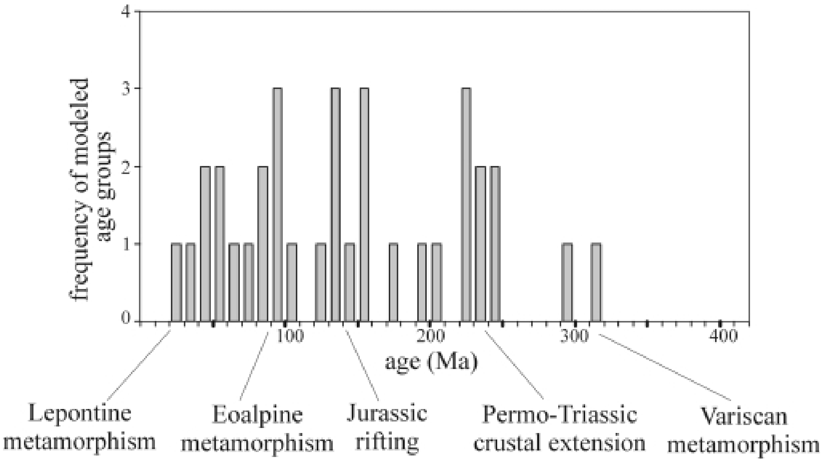

Fig. 3 Frequency of the age groups identified by the BINOMFIT program of Brandon (1992). The plot contains all age groups from all samples except those with less than five crystals.

tem (Honegg-Napf) contain zircon grains with young FT ages around 30 Myr: a 21-Myr-old sample (ZC 6) shows a small group at 32 ± 3 Myr, while a 19-Myr-old sandstone (ZC 4) yields a more pronounced age peak at 28 ± 1.2 Myr. The differences between sedimentation ages ($\sim$70 Myr) and zircon FT cooling ages ($\sim$30 Myr) points to an average cooling rate in the hinterland in the range of $\sim 20\,^{\circ}\mathrm{C}\ \mathrm{Myr}^{-1}$ for the late Oligocene to early Miocene, assuming a zircon FT closure temperature of $240 \pm 50\,^{\circ}\mathrm{C}$ (Hurford, 1986). These young age signals reflect the first exposure of Penninic basement units belonging to the hanging wall of the Lepontine Dome. The occurrence of the young age groups at $\sim$20 Ma is

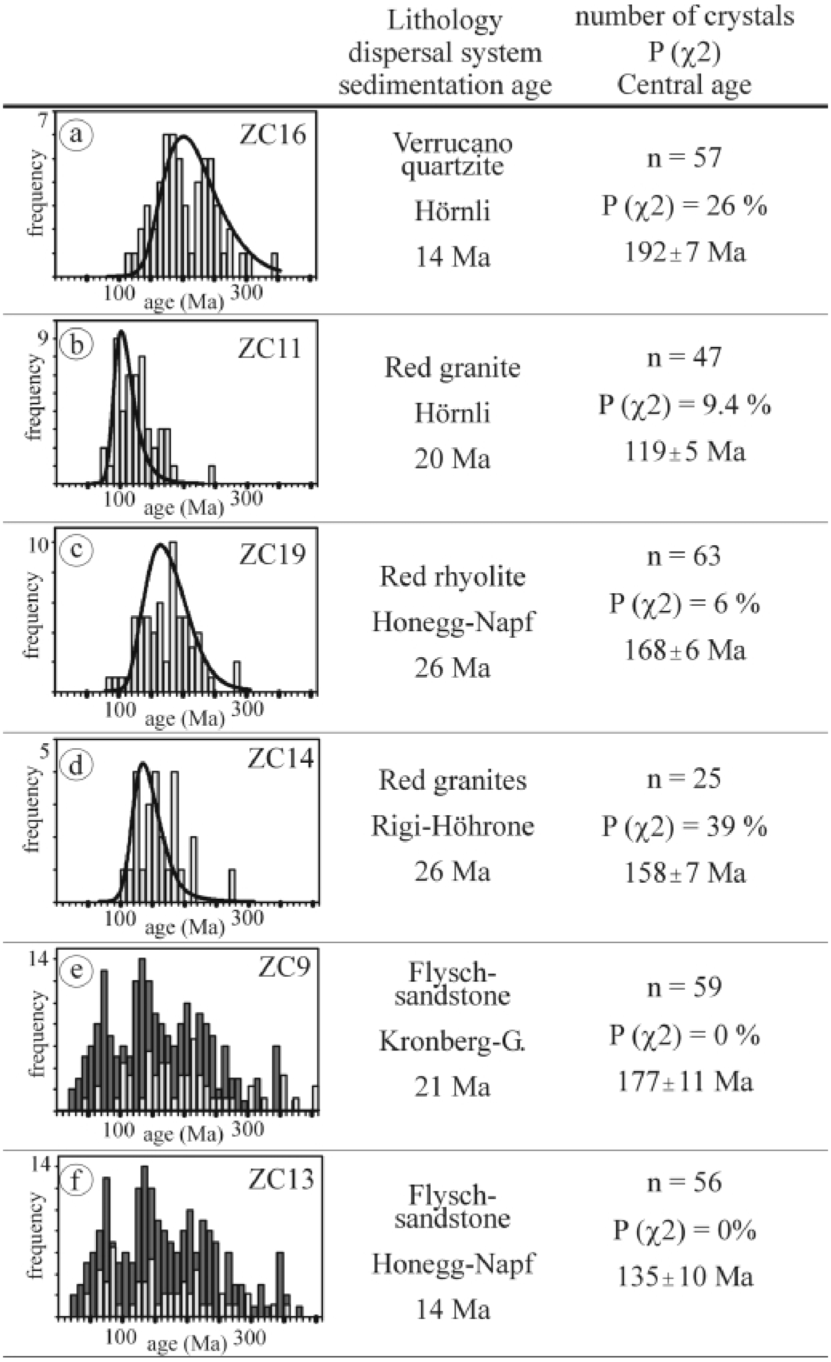

Fig. 4 Pebble population dating (PPD) results from several crystalline (a–d) and two flysch (e–f) pebble populations. For comparison, the age distributions of sandstones with sedimentation ages of 31–30 Myr are shown in 4e, f (dark-grey).

not accompanied by any sudden change in the clast composition of the conglomerates, but with a generally continuous decrease of crystalline pebbles and an increase of sedimentary pebbles from 23 until 14 Ma (Schlunegger *et al.*, 1998). This means that the increase of Penninic basement lithologies was balanced by the decrease of Austroalpine crystalline pebbles.

An early Miocene red granite pebble population (ZC 11, Fig. 4b) yields a Zr FT age of 119 ± 5 Myr, reflecting the Early Cretaceous metamorphic event (Frank *et al.*, 1987). Pebbles of the same lithotype but with Jurassic cooling ages also occur in the Oligocene molasse conglomerates (ZC 14, Fig. 4d). Thus, in early Miocene times, erosion had incised into deeper structural levels of the Austroalpine basement.

The youngest sampled molasse sandstones were deposited 14–13 Ma. Sandstones from the Honegg–Napf fan show a distinct age group of 19.5 ± 0.9 Myr (ZC 3, Fig. 2a). The difference between Zr FT age and sedimentation age of only 6 Myr yields an average cooling rate of ~40 °C Myr^{-1} in the source region for the middle Miocene. This is roughly in agreement with the middle Miocene cooling rate suggested by Hurford (1986) for the northern part of the Lepontine region and too high to be sourced from the hanging wall of the Lepontine Dome (Markley *et al.*, 1998). Therefore, at 14 Ma Lower Penninic units of the Lepontine core complex must have been exposed on the surface. At the same time a young age group of 31 ± 2 Myr occurs in the age distribution of sandstones from the Hörnli fan (ZC 12, Fig. 2b), indicating that still only upper levels of the Penninic nappe pile were eroded in the catchment area of the eastern dispersal system.

Comparison with the Miocene evolution of the Eastern Alps

The Tauern window is the largest metamorphic dome of the Eastern Alps. The first Penninic rocks derived from the Tauern window occurred at 14–13 Ma in the Austrian molasse basin (Brügel, 1998). Therefore, both metamorphic domes of the Eastern and the Central Alps were exposed contemporaneously to the surface, supporting the model that both domes were exhumed tectonically as a consequence of the Miocene lateral extrusion of the Alps (Frisch *et al.*, 2000; see also discussion in Steck and Hunziker, 1994).

In contrast to the Eastern Alps, Penninic basement units had already been exposed between 25 and 20 Ma in the Central Alps, but these units belong to the Upper to Middle Penninic hanging wall of the Lepontine Dome. The detachment between the core complexes and the hanging wall units lies in a deeper structural (intra-Penninic) level in the Central Alps, whereas in the Eastern Alps it is positioned at the Penninic–Austroalpine boundary in the present erosional level. The earlier

Table 3 Results of K–Ar dating on white mica and biotite for several crystalline pebbles

Sample Code	Lithology	Sedimentation age (Myr)	Dispersal system	Dated mineral	K (%)	^{40}Ar rad/g (ncm^3/g)	^{40}Ar rad (%)	Age (Myr $\pm$ 1σ)
CH-6/2-1	gneiss	24	Kronberg-G.	Bt	3.97	4.173×10^{-5}	79.8	252 $\pm$ 10
CH-6/2-3	granite	24	Kronberg-G.	Ms	7.21	5.285×10^{-5}	89.9	179 $\pm$ 7
CH 7	red gneiss	23	Kronberg-G.	Ms	7.85	9.111×10^{-5}	87.5	276 $\pm$ 10
CH-8/2-1	red gneiss	21	Kronberg-G.	Ms	8.2	1.047×10^{-4}	94.1	302 $\pm$ 11
CH-8/2-1	red gneiss	21	Kronberg-G.	Bt	3.28	3.616×10^{-5}	73.6	277 $\pm$ 11
CH-8/2-2	red gneiss	21	Kronberg-G.	Ms	7.67	9.498×10^{-5}	97.1	293 $\pm$ 11
CH-8/2-2	red gneiss	21	Kronberg-G.	Bt	2.24	2.671×10^{-5}	59.2	283 $\pm$ 11
CH-5/1C3	leucogranite	20	Hörnli	Ms	8.33	8.045×10^{-5}	96.4	233 $\pm$ 9

exposure of Penninic basement units in the Central Alps is in accordance with the three times higher erosion rate as compared to the Eastern Alps (Kuhlemann, 2000).

Conclusions

At the beginning of the molasse sedimentation $\sim$30 Ma mainly sedimentary cover nappes were eroded in the hinterland of the Swiss molasse basin. Until 25 Ma, erosion of Austroalpine basement nappes increases. Large parts of the eroded basement were unaffected by a Cretaceous metamorphic overprint.

At $\sim$20 Ma erosion incised into deeper levels of the Austroalpine basement and the exposure of Upper to Middle Penninic units is documented by the Zr FT age spectra. With $\sim$20 °C Myr^{-1} the cooling rate of the Penninic units was moderate. At $\sim$14 Ma the Lepontine core complex became exposed in the hinterland of the western fan. Cooling rates increased to $\sim$40 °C Myr^{-1}.

In Miocene times, the western dispersal system had their source area in deeper structural levels than the eastern dispersal systems. The exposure of the Lepontine Dome occurs contemporaneously with the exposure of the Tauern window in the Eastern Alps, indicating that both metamorphic domes were tectonically exhumed in the course of the Miocene lateral extrusion of the Alps.

Acknowledgements

This study was financed by the German Science Foundation in the frame of the Collaborative Research Centre SFB 275. Special thanks go to Oliver Kempf and Fritz Schlunegger for guidance and discussions in the field. Reviews by Tony Hurford and an anonymous reviewer are gratefully acknowledged. C. S. would like to thank Martina Schwab and Britta Trautwein for the inspiring discussions.

References

Berger, J.-P., 1992. Correlative chart of the European Oligocene and Miocene: application to the Swiss Molasse Bassin. *Eclog. Geol. Helv.*, **85**, 573–609.

Bertotti, G., Seward, D., Wijbrans, J., ter Voorde, M. and Hurford, A.J., 1999. Crustal thermal regime prior to, during, and after rifting: a geochronological and modeling study of the Mesozoic South Alpine rifted margin. *Tectonics*, **18**, 185–200.

Bolliger, T., 1992. Kleinsäugerstratigraphie in der lithologischen Abfolge der miozänen Hörnlischüttung (Ostschweiz) von MN3 bis MN7. *Eclog. Geol. Helv.*, **85**, 961–1000.

Brandon, M.T., 1992. Decomposition of fission-track grain-age distributions. *Am. J. Sci.*, **292**, 535–564.

Brügel, A., 1998. Provenances of alluvial conglomerates from the Eastalpine foreland: Oligo-/Miocene denudation history and drainage evolution of the Eastern Alps. *Tübinger Geowiss. Arb.*, **A40**.

Brügel, A., Dunkl, I., Frisch, W., Kuhlemann, J. and Balogh, K., in press. The record of Periadriatic volcanism in the Eastern Alpine Molasse zone and its paleogeographic implications. *Terra Nova*, **12**, 42–47.

Dunkl, I., Frisch, W. and Kuhlemann, J., 1999. Fission Track Record of the Thermal Evolution of the Eastern Alps – Review of the Main Zircon Age Clusters and the Significance of the 160 Ma Events. In: Abstracts of the 4th workshop on Alpine geological studies. *Tübinger Geowiss. Arb.*, A52, 77–78.

Dunkl, I., Spiegel, C., Kuhlemann, J. and Frisch, W., 2000. Impact of the volcanism on age-provenance studies – the Periadriatic event in the Alpine molasse. In: *9th International Conference on Fission Track Dating and Thermochronology* (W. Noble, P. O'Sullivan and R. Brown, eds). Geological Society of Australia abstract series 58.

Dunkl, I., Frisch, W., Kuhlemann, J. and Brügel, A., in review. Pebble-population-dating (PPD) – a new method for provenance research using single grain fission track chronology on different pebble lithologies. *Am. J. Sci.*

von Eynatten, H., 1996. Provenanzanalyse kretazischer Siliziklastika aus den Nördlichen Kalkalpen. Unpubl. doctoral dissertation, Universität Mainz.

von Eynatten, H., Schlunegger, F. and Gaupp, R., 1999. Exhumation of the Central Alps: Evidence from ^{40}Ar/^{39}Ar laserprobe dating of detrital white micas from the Swiss Molasse basin. *Terra Nova*, **11**, 284–289.

Fleischer, R.L., Price, P.B. and Walker, R.M., 1964. Fission-track ages of zircons. *J. Geophys Res.*, **69–22**, 4885–4888.

Frank, W., Kralik, M., Scharbert, S. and Thöni, M., 1987. Geochronological data from the Eastern Alps. In: *Geodynamics of the Eastern Alps*. (Flügel, H. and Faupl, P., eds), pp. 272–281. Deuticke, Vienna.

Frisch, W., Dunkl, I. and Kuhlemann, J., 2000. Postcollisional orogen-parallel large-scale extension in the Eastern Alps. *Tectonophysics*, **327**, 239–265.

Galbraith, R.F. and Green, P.F., 1990. Estimating the component ages in a finite mixture. *Nucl. Tracks Radiat. Meas.*, **17**, 197–206.

Gasser, U., 1968. Die innere Zone der subalpinen Molasse des Entlebuchs (Kt. Luzern); Geologie und Sedimentologie. *Eclog. Geol. Helv.*, **61**, 229–319.

Habicht, K., 1945. Neuere Beobachtungen in der subalpinen Molasse zwischen Zugersee und dem st. Gallischen Rheintal. *Eclog. Geol. Helv.*, **38**, 121–150.

Hunziker, J., Desmons, J. and Hurford, A., 1992. 32 years of geochronological work in the Central and Western Alps: a review on seven maps. Mém. Géol. (Lausanne), **13**.

Hurford, A., 1986. Cooling and uplift patterns in the Lepontine Alps South Central Switzerland and an age of vertical movement on the Insubric fault line. *Contr. Miner. Petrol.*, **92**, 412–427.

Hurford, A.J. and Green, P.F., 1983. The zeta age calibration of fission-track dating. *Chem. Geol., Isot. Geosci.*, **41**, 285–312.

Hurford, A.J., Fitch, F.J. and Clarke, A., 1984. Resolution of the age structure of the detrital zircon populations of two Lower Cretaceous sandstones from the Weald of England by fission track dating. *Geol. Mag.*, **121**, 269–277.

Jäger, E., 1973. Die alpine Orogenese im Lichte der radiometrischen Altersbestimmung. *Eclog. Geol. Helv.*, **66**, 11–21.

Kempf, O., Bolliger, T., Kälin, D., Engeser, B. and Matter, A., 1997. New magnetostratigraphic calibration of Early to Middle Miocene mammal biozones of the north Alpine foreland basin. In: *Actes Du Congrès Biochrom '97* (J.-P. Aguilar *et al.*, eds). *Mém. Trav. E.P.H.E., Inst. Montpellier*, **21**, 547–561.

Kuhlemann, J., 2000. Postcollisional sediment budget of circum-Alpine basins. *Mem. Sci. Geol. Padova*, **52–1**, 1–91.

Markley, M.J., Teyssier, C., Cosca, M.A., Caby, R., Hunziker, J.C. and Satori, M., 1998. Alpine deformation and $^{40}Ar/^{39}Ar$ geochronology of synkinematic white mica in the Siviez-Mischabel nappe, western Pennine Alps, Switzerland. *Tectonics*, **17**, 407–425.

Matter, A., 1964. Sedimentologische Untersuchungen im östlichen Napfgebiet (Entlebuch, Tal der grossen Fontanne, Kt. Luzern). *Eclog. Geol. Helv.*, **57**, 315–428.

Matter, A. and Weidmann, M., 1992. Tertiary sedimentation in the Swiss Molasse; an overview. *Eclog. Geol. Helv.*, **85**, 776–777.

Ruffini, R., Polino, R., Callegari, E. and Hunziker, J. and Pfeifer, H., 1997. Volcanic clast-rich turbidites of the Tavayanne sandstones from the Thone syncline (Savoie, France): records for a tertiary postcollisional volcanism. *Schweiz. Miner. Petrogr. Mitt.*, **77**, 161–174.

Schlunegger, F., Matter, A., Burbank, D. and Klaper, E., 1997. Magnetostratigraphic constraints on relationships between evolution of the central Swiss Molasse basin and Alpine orogenic events. *Bull. Geol. Soc. Am.*, **109**, 225–241.

Schlunegger, F., Slingerland, R. and Matter, A., 1998. Crustal thickening and crustal extension as controls on the evolution of the drainage network of the central Swiss Alps between 30 Ma and the present: constraints from the stratigraphy of the North Alpine Foreland Basin and the structural evolution of the Alps. *Basin Res.*, **10**, 197–212.

Schmid, S.M., Pfiffner, O.A., Froitzheim, N., Schönborn, G. and Kissling, E., 1996. Geophysical-geological transect and tectonic evolution of the Swiss-Italian Alps. *Tectonics*, **15**, 1036–1064.

Steck, A. and Hunziker, J., 1994. The Tertiary structural and thermal evolution of the Central Alps – compressional and extensional structures in an orogenic belt. *Tectonophysics*, **238**, 229–254.

Vance, J., 1999. Zircon fission track evidence for a Jurassic (Tethyan) thermal event in the Western Alps. *Mem. Sci. Geol. Padova*, **51–2**, 473–476.

Wagner, G., Miller, D. and Jaeger, E., 1979. Fission track ages on apatite of Bergell rocks from central Alps and Bergell boulders in Oligocene sediments. *Earth Planet. Sci. Lett.*, **45–2**, 355–360.

Winkler, W., Hurford, A., von Salis Perch-Nielsen, K. and Odin, G., 1990. Fission track and nannofossil ages from a Paleocene bentonite in the Schlieren Flysch (Central Alps, Switzerland). *Schweiz. Miner. Petrogr. Mitt.*, **70**, 389–396.

Received 18 May 2000; revised version accepted 23 October 2000

